Fabrication of micro and nanoparticles of paclitaxel-loaded Poly $_L$ Lactide for controlled release using supercritical antisolvent method: Effects of Thermodynamics and Hydrodynamics

Lai Yeng LEE[1], Kenneth A. SMITH[1,2], and **Chi-Hwa WANG**[1,3]

[1] MEBCS Program, Singapore-MIT Alliance, Singapore 117576
[2] Massachusetts Institute of Technology, Cambridge MA 02139
[3] Department of Chemical and Biomolecular Engineering, National University of Singapore, Singapore 117576

Abstract **– This paper presents the fabrication of controlled release devices for anticancer drug paclitaxel using supercritical antisolvent method. The thermodynamic and hydrodynamic effects during supercritical antisolvent process on the particle properties obtained were investigated. Scanning electron microscopy was employed to study particle sizes and morphologies achieved. It was observed that increasing supercritical pressure improves the surface morphology of particles obtained, and increasing the flow rate of the organic solution jet reduces the particle sizes obtained. A modified Supercritical Antisolvent with Enhanced Mass transfer setup was developed to produce monodispersed nanoparticles with high recovery yield. High performance liquid chromatography was used to determine the encapsulation efficiency and *in vitro* release profiles of paclitaxel loaded particles obtained. The encapsulation efficiencies of particles obtained using the modified SASEM process were high and up to 83.5%, and sustained release of paclitaxel from the polymer matrix was observed over 36 days release. The thermogram properties of the particles were also analyzed using differential scanning calorimetry to determine the crystalline state of polymer and drug.**

Index terms – supercritical antisolvent, controlled release devices, paclitaxel, Poly $_L$ lactide, ultrasonication

I. Introduction

Particle formation is an important application of supercritical fluid technology [1]. Favorable properties of supercritical fluids for particle formation include liquid-like density and gas-like viscosity [2]. The well known techniques for particle formation using supercritical fluids include the rapid expansion of supercritical solutions (RESS) [1 – 4] and the supercritical antisolvent (SAS) processes [1 – 3, 5 – 13]. The most commonly used supercritical fluid in pharmaceutical applications is CO_2, which is attributed to its desirable properties such as relatively accessible critical point (Tc = 31.1 ^oC, Pc = 73.8 bars), abundance and its low toxicity [1 – 3]. Since most organic solvents are miscible with CO_2 at supercritical conditions, a low residual solvent content can be easily achieved in the final product without extensive downstream purification to remove excess organic solvent [14].

Several factors may affect the particle size and properties achieved from SAS process. This includes the phase behavior of the ternary mixture, the hydrodynamics of the solution injected into the supercritical phase, as well as the thermodynamic conditions of the supercritical fluid. Considerable literature suggests that the controlling parameter for particle size in the SAS process is the rate of mass transfer [12, 13]. This may be influenced by both the spray hydrodynamics and thermodynamic properties of the supercritical fluid phase. Diego et al. [15] reported the mechanism of particle formation in subcritical and supercritical regimes for precipitation from compressed antisolvent (PCA) process. The jet breakup for operation in subcritical and supercritical conditions was different and hence particles properties were different. The effect of flow rate on particle size in the subcritical regime was reported. Carretier et al. [16] investigated the hydrodynamics of the SAS process by evaluating the macro and micromixing within the precipitation vessel. Varying liquid flow rates were studied for their effect on jet breakup lengths and particle properties. It was shown that fibers or microparticles may be obtained in their studies depending on liquid flow rate. Similar studies have been carried out to investigate the influence of enhanced mixing of the spray jet with supercritical CO_2 using coaxial nozzles [13] and ultrasonic nozzles [5, 6]. These processes were found to yield smaller and more uniform sized particles as compared to conventional SAS. Chattopadhyay and Gupta [7 – 11] used an ultrasonic vibrating surface to break up the solution jet into smaller droplets and also increase the mass transfer rates between supercritical CO_2 and organic solvent. This has been termed the supercritical antisolvent with enhanced mass transfer process (SASEM).

In this study, SAS and a modified SASEM process was developed to fabricate micro and nanoparticles of a biodegradable and biocompatible polymer Poly $_L$ lactide

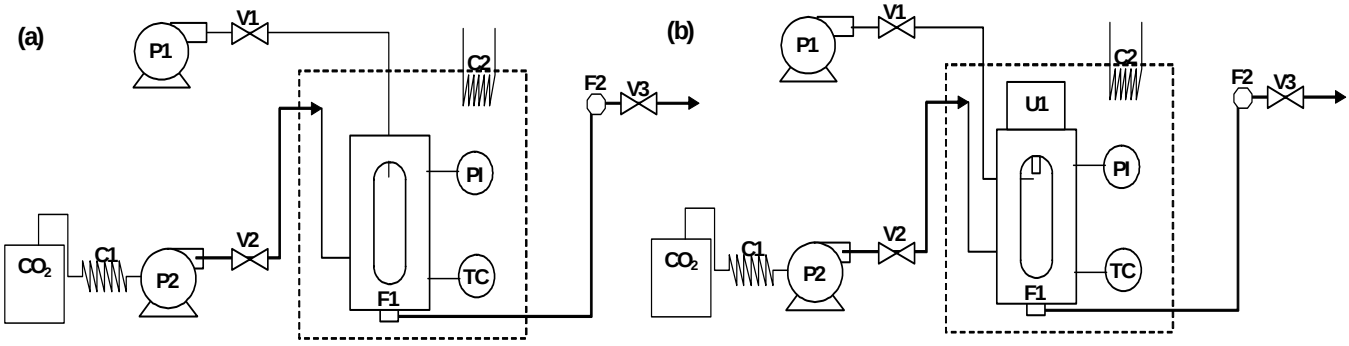

Fig. 1. Experimental setup for (a) Supercritical antisolvent (SAS) production of micro and nanoparticles of PLA
(b) Modified supercritical antisolvent with enhanced mass transfer (SASEM) setup

HP: Jerguson 12-T-32 high pressure vessel (For supercritical antisolvent process); U1: Ultrasonic system; Branson sonifier and converter, Sonics and Materials probe (3/8" probe tip diameter); C1: Polyscience 912 refrigerating circulator (for liquefying CO_2); C2: Polyscience 712 circulator with temperature control (Water bath); P1: Eldex B-100-S HP series pump (for solution injection); P2: Jasco HPLC pump (for pumping liquefied CO_2 into HP vessel); F1: 0.22 micron filter membrane (to collect particles from bottom of vessel); F2: stainless steel filter (0.22 micron, for filtering the contents leaving the vessel); V1: Swagelok 1/16" tube connection ball valve (solution line);V2: Swagelok 1/16" tube connection ball valve (CO_2 line); V3: Swagelok 1/8" tube connection ball valve (to vent); TC: Thermocouple connected to Thermometer read out; PI: Swagelok Pressure gauge

(PLA). The main difference between the modified process and the usual SASEM process is that the organic solution spray was directed away from the ultrasonic vibrating surface. The atomization of the inlet solution was achieved by jet breakup at supercritical pressures and not due to ultrasonic liquid atomization of a liquid level at the vibrating surface. The ultrasonic probe is fitted into the high pressure vessel to create extensive mixing and turbulence within the vessel during the modified SASEM process. The organic solution was introduced into the high pressure vessel through a 500 μm ID stainless steel capillary. The high pressure vessel has borosilicate glass windows which allow observation of the SAS and the modified SASEM process.

II. Materials and Methods

A. Materials

Poly (L-lactic acid) (PLA, Product Number P1566, MW = 85,000 – 160,000 Da) was purchased from Sigma Aldrich. polyethylene glycol (PEG, Product number P4463, Typical MW = 8,000 Da) were purchased from Sigma Aldrich. Paclitaxel was a generous gift from Bristol Myers Squibb. Compressed CO_2 (Alphagaz) was purchased from Soxal (Singapore Oxygen Air Liquide Pte Ltd). Dichloromethane (DCM, Product Number DS1432, HPLC/Spectro Grade) and acetonitrile (ACN, Product Number AS1122, HPLC/Spectro Grade) were purchased from Tedia (Tritech Scientific Pte Ltd, Singapore). Phosphate buffered saline (PBS) was purchased from Sigma Aldrich (pH = 7.4). Millipore water was used throughout the study.

B. Microparticles and nanoparticles preparation

The experimental equipment for the SAS and modified SASEM processes is shown in Figure 1a and 1b respectively. Table 1 summarizes the main differences between the present setup and the SASEM process. Paclitaxel and PLA were first dissolved in DCM. Theoretical drug to polymer loadings of 5 and 10% (w/w), and polymer to solvent loadings of 1 and 2% (w/v) were used in the experiments performed.

The high pressure vessel was first purged and filled with compressed CO_2 (50 – 60 bars). Liquefied CO_2 was subsequently pumped into the vessel by a high pressure pump to attain the required pressure. The temperature in the vessel was controlled by use of a heated water bath. Ultrasonic vibration amplitude of 0 – 90 μm was used in the experiments with modified SASEM setup. The organic solution was pumped into the high pressure vessel at a flow rate of 2 to 6 ml/min through a capillary tubing of ID 500μm.

After the batch precipitation process, the DCM-CO_2 mixture was vented off to a fume cupboard. Fresh CO_2 was introduced into the vessel at 50 bars for 3 times to remove any residual DCM in the particles. The particles were collected at the bottom of the vessel on a 0.22 μm cellulose acetate filter during the venting process.

C. Size and Surface morphology analysis

Qualitative observation of the size and surface morphology of the particles was achieved by scanning electron microscopy (SEM) (JEOL JSM-5600 LV). Platinum coating (Autofine Coater, JEOL JFC-1300) of the samples was required before SEM analysis. The particle size and size distribution was determined using SMILEVIEW software on the SEM pictures captured.

D. Thermogram properties analysis

Phase behavior of the particles was studied by differential scanning calorimetry (DSC) (2920 modulated,

TABLE 1.
Summary of differences between modified SASEM setup in present study and SASEM.

	Present study (Modified setup)	SASEM
High pressure cell volume	68.4 ml	80.0 ml
Organic phase feeding system	HPLC reciprocating pump	High pressure piston device
Sonicator	Maximum 400W Probe tip 0.825mm	Maximum 600W Probe tip 1.25mm
Capillary ID	500 mm (stainless steel)	75 mm (fused quartz)
Solvent removal	CO2 – solvent solution removed from bottom of vessel	CO2 – solvent solution removed from side of vessel
Spray jet	Jet directed away from sonicator vibrating surface (Horizontal jet)	Capillary placed against the probe surface

Universal V2.6D TA instruments). Approximately 2-10 mg of particles was loaded onto standard aluminum pans (40mg) with lids. The samples were purged with pure dry nitrogen at flow rate of 5 ml/min. A blank aluminum pan was used as reference in all the experiments. The analysis was carried out using a temperature ramp of 10 ^{o}C/min from 20 – 280 ^{o}C.

E. Encapsulation efficiency and in vitro release profile

High pressure liquid chromatography (HPLC) (Agilent HPLC Series 1100 with UV-visible detectors) was used to determine the encapsulation efficiency and in vitro release profile of the paclitaxel-loaded PLA particles. An acetonitrile : water (50 : 50 v/v%) solution was used as the mobile phase.

Encapsulation efficiency of each paclitaxel-loaded sample was carried out in triplicate. Approximately 0.5 mg of sample was weighed and dissolved in 0.5ml DCM to extract the paclitaxel embedded in the polymer matrix. After all the DCM has evaporated, 5ml of mobile phase was added and placed in an ultrasonic water bath to dissolve the paclitaxel in the mobile phase. Subsequently, 2ml of the solution was filtered (0.22μm syringe filters) into HPLC vials for analysis. The HPLC column was calibrated for peak area at paclitaxel concentrations of 1, 5, 10, 40, 60, 80 and 100 μg/ml in the mobile phase.

The in vitro release profile was also determined in triplicate. Approximately 5mg of each sample was weighed and suspended in 6ml PBS and placed into a shaking water bath (120 rpm) at 37 ^{o}C to mimic physiological conditions. At predetermined time intervals, the solution was centrifuged at 11500 rpm for 30min. After centrifugation, 5ml of the supernatant was removed and 5ml of fresh PBS was added to the particles to re-suspend them. The paclitaxel content in the supernatant was extracted into 1ml DCM. The DCM with paclitaxel was then left to evaporate before addition of 2ml of the mobile phase which was subsequently filtered into HPLC vials for similar analysis as described for encapsulation efficiency.

III. RESULTS AND DISCUSSION

Many factors play a role in manipulating the particle formation during the SAS process. It was reported that the influencing factor in SAS is the extent of mixing and mass transfer between the solvent – antisolvent phases [12 – 13]. The thermodynamics and hydrodynamics effect on particle formation in SAS process is investigated in this study.

A. Thermodynamics effect

The diffusivity and viscosity are transport properties that affect mass transfer rates. Diffusivity in supercritical fluids is higher than a liquid solvent and hence a solid will dissolve more rapidly in a supercritical fluid. Diffusion coefficient of a supercritical fluid varies with temperature and pressure, and strongly influenced by density and viscosity [17]. In pharmaceutical applications, it is necessary to maintain low processing temperatures in order to prevent degradation of pharmaceutics. Therefore, we are interested to determine the effects of varying pressure on the particle formation process at a constant low processing supercritical temperature of 35 ^{o}C.

SAS process was carried out at pressures of 73.8 bars (Critical pressure of CO_2), 80 bars, 90 bars and 95 bars respectively. Figure 2a and b shows the particles obtained at 73.8 and 80 bars respectively. Microparticles were obtained for both cases. It was observed at these near-critical conditions, the particles obtained had very rough surfaces. The particles obtained at 73.8 bars appear to be slightly agglomerated.

At higher pressures, it was observed that particles obtained were less agglomerated. Figure 3a and 3b shows the particles obtained at 90 and 95 bars respectively. Figure 3c and 3d shows the close up of the surface morphologies for the particles in 3a and 3b respectively.

In all 4 cases for varying pressure, microparticles of approximately 5-10 μm were obtained. The differences in surface morphology suggest a difference in the solvent removal rate during the SAS process. The rate of solvent removal is dependent on the miscibility of the organic solvent and antisolvent phases. The agglomeration of particles obtained at 73.8 bars may be due to the slower solvent removal rate as compared to higher pressures. Significantly less agglomeration was observed for pressures higher than 80 bars.

B. Hydrodynamics effect

The hydrodynamics have been found to influence particle morphologies [16]. In this study, the hydrodynamics of the SAS process was investigated by varying the liquid flow rates of the organic phase and also by application of ultrasonic vibration to the supercritical CO_2 phase during the precipitation step. Varying liquid flow rates of the organic phase were applied to the SAS process at 90 bars and 35 ^{o}C to determine the relationship between flow rates and particle properties. Figure 4 shows

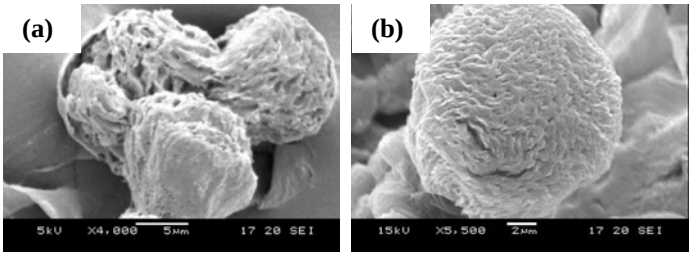

Fig. 2. Representative SEM images of paclitaxel loaded PLA particles obtained from SAS at (a) 73.8 bars; (b) 80 bars

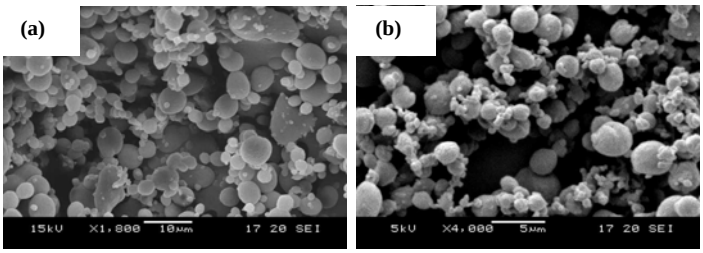

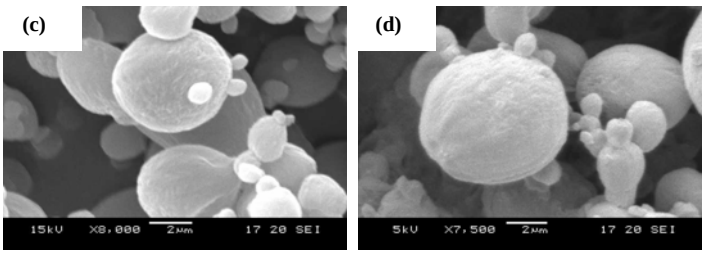

Fig. 3. Representative SEM images of paclitaxel loaded PLA particles obtained from SAS at (a) 90 bars; (b) 95 bars; (c) close up of particle surface for (a); (d) close up of particle surface for (b).

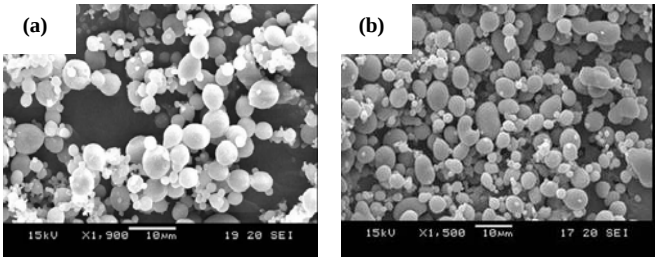

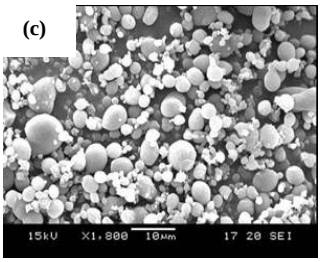

Fig. 4. Representative SEM images of paclitaxel loaded particles obtained from SAS at liquid flow rate of (a) 2 ml/min; (b) 4 ml/min; (c) 6 ml/min

TABLE 2.
Paclitaxel loaded PLA samples obtained using modified SASEM process

Sample	Ultrasonic vibration amplitude (μm)	Recovery Yield (%)	Encapsulation efficiency (%)	Size (nm)
S1	0	21.1	70.0 ±3.5	4130 ± 198
S2	30	18.1	67.7 ± 1.4	769 ± 210
S3	60	14.6	56.4 ± 14.4	506 ± 163
S4	90	12.8	83.5 ± 0.8	486 ± 134

the SEM images of particles obtained at flow rates of 2, 4 and 6 ml/min.

From the SEM images, no significant differences were observed for particle size and morphology. However, upon careful observation, it was found that the particles may be divided into 2 main size clusters. Particles of around 1 μm and particles of around 2-10 μm. Figure 5 shows the size distribution of particles from liquid flow rates of 4 ml/min and 6 ml/min. Particles around 1 μm and particles around 2-10 μm in size. Figure 5 shows the size distribution of particles from liquid flow rates of 4 ml/min and 6 ml/min. For both particle size distribution curves, a peak at approximately 1 μm was observed. However, at 6ml/min the second peak is at a smaller size then the corresponding one for 4ml/min. The overall mean and standard deviation of the particle size for samples from 6 ml/min is lower than the samples from 4 ml/min. The larger particles may be formed as a result of growth of particles from few particles during the precipitation process. Higher liquid flow rate enhances the mixing of the jet with the supercritical CO_2 and hence reduces the size of particles.

The application of ultrasonication during the SAS process was also evaluated. This process is similar to the SASEM process reported by Chattopadhyay and Gupta [7 – 11]. The main difference of the present setup is in the horizontal jet for organic phase instead of directing the jet at the ultrasonic probe vibrating surface. Figure 6 is a photograph taken of the jet breakup and mixing during the modified SASEM process used in present setup. The size and morphologies of particles obtained from SAS and modified SASEM were illustrated in Figure 7.

The particle size is significantly reduced by the application of ultrasonication. Nanoparticles with much narrow size distribution were achieved using the modified SASEM setup. The recovery yield and sizes of particles obtained were summarized in table 2. The yield was 12.8% to 21.1% which is comparable to the yield for spray drying methods [18]. The main advantage of SAS over spray drying is the rapid removal of organic solvent without the need for high temperatures. The encapsulation efficiency of paclitaxel in the micro and nanoparticles fabricated using SAS/SASEM was very high up to 83.5%.

C. Applications for controlled release

The nanoparticles obtained using the modified SASEM process was further evaluated for their suitability for controlled release applications. The encapsulation and sustained release of a hydrophobic anticancer drug, paclitaxel, was employed to characterize the properties and release from PLA micro and nanoparticles. Paclitaxel is a promising anticancer drug with efficacy against a wide

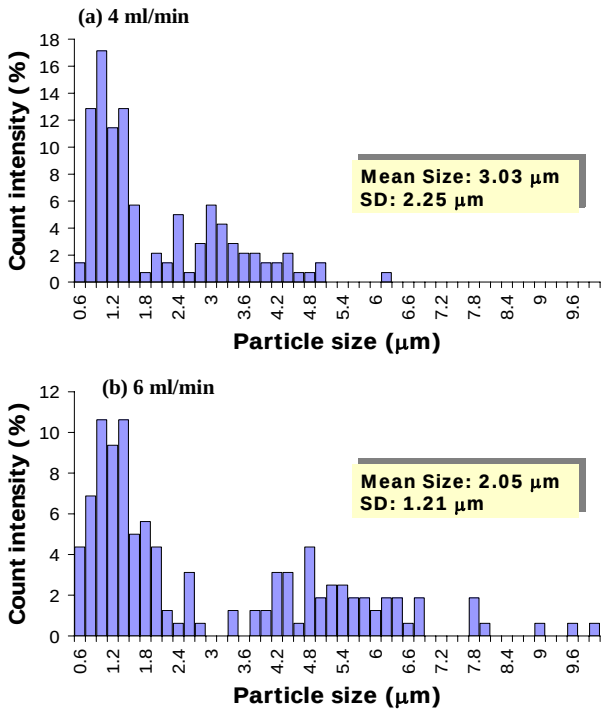

Fig. 5. Particle size distribution obtained from liquid flow rates of (a) 4 ml/min; (b) 6 ml/min.

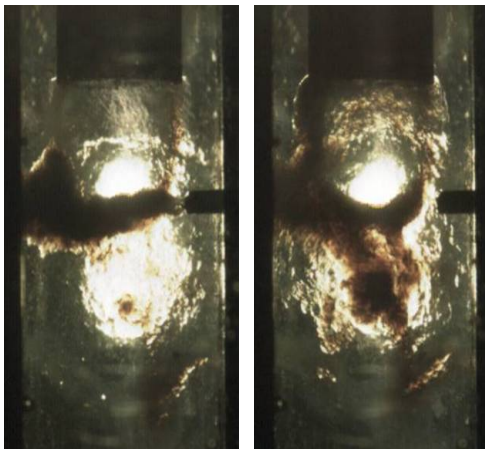

Fig. 6. High resolution photograph of modified SASEM process. The organic enters the high pressure vessel as a gaseous plume. The mixing between solvent and antisolvent is improved by the ultrasonic vibration.

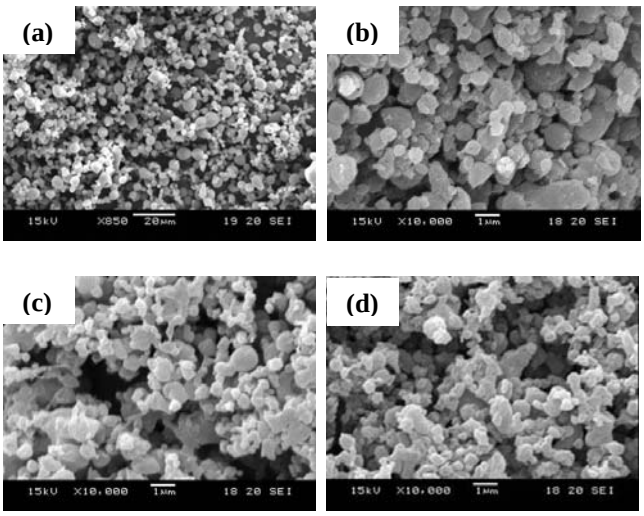

Fig. 7. Representative SEM images of paclitaxel loaded PLA particles obtained at varying ultrasonic vibration amplitude (a) No ultrasonication; (b) 30 μm vibration amplitude; (c) 60 μm vibration amplitude; (b) 120 μm vibration amplitude. Note the difference in scale for Fig. 7a with Fig 7b-7c.

variety of carcinomas [18 – 24]. It works through the inhibition of DNA synthesis by stabilizing microtubule assembly [19]. However, its clinical application has been limited due to its hydrophobic nature. Its current formulation requires the use of an adjuvant, Cremophor® EL, which has been associated with several undesirable side effects [19, 21 – 24]. One method to overcome the problems brought about by Cremophor® EL is to encapsulate paclitaxel in biodegradable polymers such PLA or poly (DL lactic-co-glycolic acid) (PLGA) in micro and nanoparticles. These biodegradable polymeric particles also have the advantage of providing sustained release of paclitaxel for chemotherapy [18, 21 – 24].

The thermal properties, encapsulation efficiency and in vitro release profiles of the paclitaxel loaded PLA particles fabricated were studied. Thermal analysis is a useful tool for examine the dispersion of drugs in polymeric microsphere matrix [25, 26]. The thermogram properties of the particles fabricated in this study was analyzed using the differential scanning calorimetry (DSC). The exotherm for the paclitaxel and PLA used in this study are shown in Figure 8. Pure paclitaxel has a characteristic endothermic peak at approximately 223.0 ^{o}C [27] and the DSC analysis shows paclitaxel with an endothermic peak at 224.5 ^{o}C which is in close agreement with the literature value. The melting peak for pure PLA before processing was 178.7 ^{o}C.

The thermogram analysis of the drug-encapsulated microparticles and nanoparticles allow us to determine whether most of the paclitaxel was molecularly dispersed in the polymer matrix or crystallized out as needles during the precipitation process. In Figure 8, the exotherm for blank PLA (without paclitaxel) and PLA (with 10% paclitaxel) fabricated using the supercritical antisolvent process were illustrated. The endothermic melting peak for the blank PLA particles was 175.8 ^{o}C which was approximately 3 ^{o}C lower then the untreated PLA particles. It was also observed that, with paclitaxel-loaded particles, the endothermic peak is further shifted by approximately 2 ^{o}C.

The supercritical antisolvent process with ultrasonication did not significantly alter the polymeric structure for PLA. There was also no endothermic peak observed for the paclitaxel-loaded particles exotherm in the vicinity of 220 – 230 ^{o}C, i.e., near the melting point of paclitaxel. Therefore, we can deduce that, in the fabrication of the paclitaxel-loaded PLA particles, there was no significant phase separation and no crystalline paclitaxel was present at 10% drug loading.

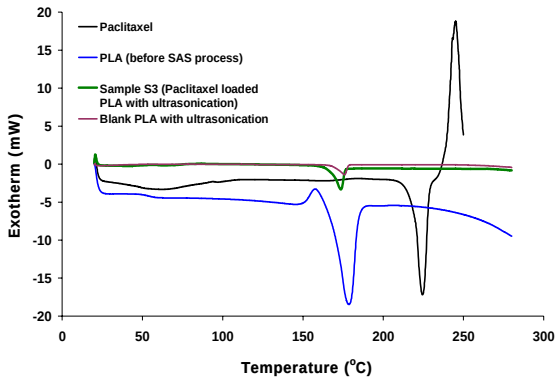

Fig. 8. Thermogram properties for raw materials used and nanoparticles fabricated using the modified SASEM process.

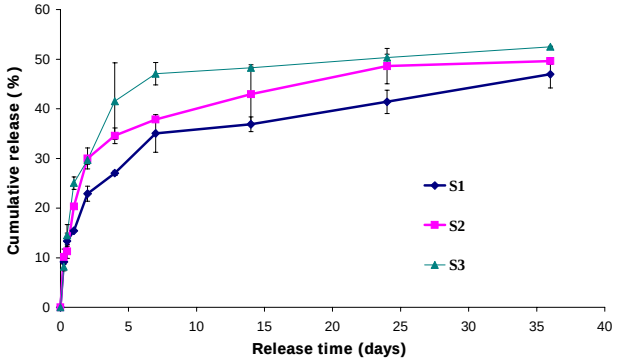

Fig. 9. In vitro release profiles of paclitaxel loaded particles fabricated using modified SASEM process with ultrasonic vibration amplitude 0 – 60 μm.

The in vitro release profiles of the 10% paclitaxel samples fabricated at varying ultrasonic vibration amplitude were determined and are illustrated in Figure 9. In vitro release profiles of the paclitaxel-loaded particles were determined for up to 36 days release. As shown in Figure 9, the release of paclitaxel from S1 (sample prepared with no ultrasonic vibration) had an initial burst of 20% cumulative release in the first 2 days. The corresponding initial burst was approximately 30% for samples S2 and S3. Beyond the 5th day of in vitro release, the release profiles of samples S2 and S3 seemed to be similar. The initial burst is primarily due to the diffusion out of paclitaxel close to the surface of the particles. Since particle sizes for samples S2 and S3 were much smaller than S1, it was reasonable to observe an increase in initial release profile with decrease in particle size. Subsequent release of paclitaxel from the polymer matrix is dependent upon the bulk erosion of the polymer. Since the polymer matrixes for all the samples were similar, the bulk erosion process is similar and hence the explanation for similar release profiles beyond 5th day of in vitro release. Further studies will be carried out to explain the release behavior in greater detail.

IV. Conclusions

Both thermodynamics and hydrodynamics effects of the SAS process was examined in this study. An increase in pressure from critical to supercritical conditions enhanced the surface morphology of particles achieved. The hydrodynamics was evaluated by studying the effects of varying liquid flow rates and ultrasonic vibration amplitude. In this study, it was observed that both size and size distribution are dependent on the hydrodynamics of the SAS process. The synergistic effect of combining flow rate and ultrasonic vibration amplitude for particle size control will be further evaluated in near future studies.

The modified SASEM process has been applied successfully for fabricating PLA nanoparticles with paclitaxel loading for sustained release. The in vitro release profile of the samples show sustained release of paclitaxel for up to 36 days.

Acknowledgements

This research is supported by research grant C382-427-003-091. The authors would like to thank Prof Yee C. Chiew and Dr Zhen Huang for their technical support in this work. The authors would also like to thank Prof Jefferson W. Tester (MIT, USA), Mr Jingwei Xie and Dr Michael T. Timko for their most helpful discussions in this study and Mr Brian Moyer (Thartech) for providing advice on the technology.

References

[1] J. Jung and M. Perrut, "Particle design using supercritical fluids: Literature and patent survey" *J. Supercritical Fluids*. 20, pp 179 – 219, 2001.

[2] J. Richard and F. S. Dechamps, "Supercritical Fluid Processes for Polymer Particle Engineering – Applications in the Therapeutic Area", in Colloidal biomolecules, *biomaterials, and biomedical applications – edited by A. Elaissari*. New York: M. Dekker, 2004, pp 429 – 475.

[3] J. W. Tom and P. G. Debenedetti, "Particle Formation with Supercritical Fluids – A review". *J. Aerosol. Sci*. 22, pp 555 – 584, 1991

[4] P. G. Debenedetti, J.W. Tom and S. D. Yeo, "Rapid expansion of supercritical solutions (RESS): Fundamentals and Application" *Fluid Phase Equilibria*. 82, pp 311 – 321, 1993

[5] T. W. Randolph, A.D. Randolph, M. Mebes and S. Yeung, "Sub-micrometer-sized biodegradable particles of poly (L-lactic acid) via the gas antisolvent spray precipitation process" *Biotechnol. Prog.* 9, pp 429 – 435, 1993

[6] B. Subramaniam, S. Saim, R. A. Rajewski, and V. Stella, "Methods for a particle precipitation and coating using near-critical and supercritical antisolvents" *Patent No. 5,833, 891*, 1997

[7] P. Chattopadhyay and R B. Gupta, "Production of antibiotic nanoparticles using supercritical CO_2 as antisolvent with enhanced mass transfer" *Ind. Eng Chem. Res.* 40, pp 3530 – 3539, 2001

[8] P. Chattopadhyay and R B. Gupta, "Production of griseofulvin nanoparticles using supercritical CO_2 antisolvent with enhanced mass transfer" *Int. J. Pharma.* 228, pp 19 – 31, 2001

[9] P. Chattopadhyay and R B. Gupta, "Protein nanoparticles formation by supercritical antisolvent with enhanced mass transfer" *AIChE Journal*. 48 (2), pp 235 – 244, 2002

[10] P. Chattopadhyay and R B. Gupta, "Supercritical CO_2 based production of magnetically responsive micro- and nanoparticles for drug targeting" *Ind. Eng. Chem. Res*. 41, pp 6049 – 6058, 2002

[11] P. Chattopadhyay and R B. Gupta, "Methods of forming nanoparticles and microparticles of controllable size using supercritical fluids and ultrasound". *Pub. No. 2002/0000681*, 2002

[12] E. Reverchon, G. Caputo and I. De Marco, "Role of phase behavior and atomization in the supercritical antisolvent precipitation" *Ind. Eng. Chem. Res*. 42, pp 6406 – 6414, 2003

[13] M. Henczka, J. Baldyga, B. Y. Shekunov, “Particle formation by turbulent mixing with supercritical antisolvent”, *Chem. Eng. Sci.* 60, pp 2193 – 2201, 2005

[14] F. Ruchatz, P. Kleinebudde and B. W. Muller, “Residual solvent in biodegradable microparticles: Influence of process parameters on the residual solvent in microparticles produced by the aerosol solvent extraction system (ASES) process”, *J. Pharma. Sci.* 86 (1), pp 101 – 105, 1997.

[15] Y. Perez de Diego, H. C. Pellikaan, F. E. Wubbolts, G. J. Witkamp and P. J. Jansens, “Operating regimes and mechanism of particle formation during the precipitation of polymers using the PCA process”, *J. Supercritical fluids*, 35, pp 147 – 156, 2005

[16] E. Carretier, E. Badens, P. Guichardon, O. Boutin and G. Charbit. “Hydrodynamics of supercritical antisolvent precipitation: Characterization and influence on particle morphology”, *Ind. Eng. Chem. Res*. 42, pp 331 – 338, 2003

[17] F. P. Lucien and N. R. Foster, “Phase Behavior and Solubility” in Chemical Synthesis using supercritical fluids – edited by P. G. Jessop and W. Leitner. (1999) Wiley-VCH, pp 37-53.

[18] L. Mu, S.S. Feng, “Fabrication, characterization and in vitro release of paclitaxel (Taxol ®) Poly (DL-lactic-co-glycolic acid) microspheres prepared by spray drying technique with lipid/ cholesterol emulsifiers”. *J. Control. Rel*. 76, pp 239 – 254, 2001

[19] A. K. Singla, A. Garg and D. Aggarwal, “Paclitaxel and its formulations”, *Int. J. Pharma*. 235, pp 179 – 192, 2002

[20] R. B. Ewesuedo, M. J. Ratain, Systemically administered drug, Drug Delivery systems in cancer therapy, edited by D. M. Brown (2004) pp 3 – 13, Humana press

[21] L. Mu, S. S. Feng, PLGA/TPGS Nanoparticles for controlled release of paclitaxel, *Pharma. Res.* 20, pp 1864 – 1972, 2003

[22] L. Mu, S. S. Feng, “A novel controlled release formulation for the anticancer drug paclitaxel (Taxol®): PLGA nanoparticles containing vitamin E TPGS”, *J. Control. Rel*. 86 (2003) pp 33 – 48, 2003

[23] S. S. Feng, L. Mu, K. Y. Win, G. Huang, “Nanoparticles of biodegradable polymers for clinical administration of paclitaxel”, *Curr. Med. Chem.* 11, pp 413 – 424, 2004

[24] J. Wang, C. W. Ng, K. Y. Win, P. Shoemakers, T. K. Y. Lee, S. S. Feng, C. H. Wang, “Release of paclitaxel from polylactide-co-glycolide (PLGA) microparticles and discs under irradiation”, *J. Microencapsulation.* 20, pp 317 – 327, 2003

[25] C. Dubernet, “Thermoanalysis of microspheres”, *Thermochimica Acta*, 245, pp 259 – 269, 1995

[26] O. I. Corrigan, “Thermal analysis of spray dried products”, *Thermochimica Acta*, 248, pp 245 – 258, 1995

[27] R. T. Liggins, W. L. Hunter, H. M. Burt, “Solid state characterization of paclitaxel’, *J. Pharma. Sci,* 86, pp 1458 – 1463, 1997